10th International Conference on Fracture Mechanics of Concrete and Concrete Structures
FraMCoS-X
G. Pijaudier-Cabot, P. Grassl and C. La Borderie (Eds)
https://doi.org/10.21012/FC10.232063

ASSESSMENT OF FIRE EXPOSED CONCRETE WITH FULL-FIELD STRAIN DETERMINATION AND PREDICTIVE MODELLING

N. WILLIAMS PORTAL[*] AND M. FLANSBJER[*]

[*] RISE Research Institutes of Sweden
501 15, Borås, Sweden
e-mail: natalie.williamsportal@ri.se, mathias.flansbjer@ri.se www.ri.se

Key words: Concrete, Fire, Damage Assessment, Digital Image Correlation, Finite Element Analysis

Abstract: A condition assessment of civil engineering structures is typically performed after the occurrence of a fire incident to determine the remedial actions required out of a structural point of view. A condition assessment is based on the mapping of damage on the given structure, which is traditionally executed via methods that yield indirect results related to surface and/or geometric properties. To be able to predict the accurate fire resistance performance of a given structure, it is most suitable to apply a mapping method which can be directly coupled to the change in material properties of concrete at high temperatures. The aim of this study is to explore the potential of applying an innovative damage mapping methodology directly coupled to the change in material properties of concrete at high temperatures. This methodology consists of optical full-field strain measurements based on Digital Image Correlation (DIC) coupled with a predictive model based on finite-element analysis (FEA). An experimental study was firstly conducted to expose concrete slabs to a standard fire curve. Subsequently, compression tests were performed on drilled cores taken from the damaged induced specimens, all while optically measuring the full-field strain on a specimen surface. As a preliminary step, an FE model of a fire exposed core was developed based on input data from standard temperature-dependent properties. The analysis consisted of a sequentially coupled thermal stress analysis to solve the multiphysics problem. The model was able to capture the temperature distribution in the concrete with enough certainty given the choice of input data. The resulting strain along the height of the core was also comparable to the experimental optical strain measurements, particularly as the distance increased from the fire exposed surface. These results can be practical when assessing the required strengthening actions to restore the load carrying capacity and durability of the concrete structure.

1 INTRODUCTION

Concrete is known to be the most employed building material in construction. Due to its versatility, it is applied in a wide range of structures and infrastructures, such as residential and commercial buildings, dams, roads, bridges and tunnels. Concrete is inexpensive, durable and has satisfactory fire performance in most cases of fire exposure. Despite this fact, serious damage or even collapse could occur in certain circumstances.

After the occurrence of a fire incident, it is important to perform a condition assessment of civil engineering structures to determine the remedial actions required out of a structural point of view. The refurbishment of the damaged structure is the recommended alternative compared to demolition, as this could result in substantial economic and time

savings. A condition assessment is based on the mapping of damage on the given structure, which is traditionally executed via e.g. rebound hammer, ultrasonic pulse measurements and microscopy methods. The primary limitation of these methods is such that they yield indirect results related to surface and/or geometric properties. To be able to predict the accurate fire resistance performance of a given structure, it is most suitable to apply a mapping method which can be directly coupled to the change in material properties of concrete at high temperatures.

The aim of this study is to investigate the potential of applying an innovative damage mapping methodology consisting of optical full-field strain measurements based on Digital Image Correlation (DIC) coupled with a predictive model based on finite-element analysis (FEA). DIC has been shown to be a promising method to study the compressive strains of concrete exposed to elevated temperatures [1, 2].

Experiments consisting of exposing concrete slabs to a standard fire curve as per ISO 834-1 [3] were firstly conducted. Subsequently, compression tests were performed on drilled cores taken from the damaged induced specimens to determine the degree of degradation along the height with respect to the compressive properties. During compressive testing, the mechanical response at different specimen heights was captured using optical full-field strain measurements.

As a first trial, an FE model of a fire exposed core was developed based on input data from standard temperature-dependent properties, see EN 1992-1-2 [4]. The analysis consisted of a sequentially coupled thermal stress analysis to solve the multiphysics problem, such that an uncoupled heat transfer analysis was firstly conducted followed by a stress/deformation analysis. The validation of the predictive model is achieved by comparing the experimental and numerical results.

2 EXPERIMENTAL STUDY

The experimental study consisted of evaluating the level of damage of fire exposed concrete using a full-field strain measuring technique based on DIC. The first stage of the study consisted of exposing concrete slabs to a standard fire curve as per ISO 834-1 [3]. Subsequently, compression tests were performed on drilled cores taken from the damaged induced specimens to determine the degree of degradation. The mechanical response at different specimen heights was captured using DIC during testing.

2.1 Material and specimen description

A typical Swedish tunnel concrete was investigated in this study with the incorporation of differing aggregate sizes, so-to-say 0-8 mm and 0-16 mm. By doing so, the influence of aggregate size on the degradation of the fire exposed concrete could be studied. Moreover, polypropylene (PP) fibers were added to the respective mixes to reduce fire spalling during testing. The concrete mix proportions are provided in Table 1.

Table 1: Concrete mix proportions.

Constituents [kg/m^3]	Mix 0-8	Mix 0-16
w/c	0.47	0.45
Gravel, 0-8 mm	1637.8	898.5
Gravel, 0-16 mm	-	863.3
Water	181.1	180.9
Cement, CEM I	385.5	402.8
Superplasticizer	0.72%	0.16%
PP-fibers	1.0	1.0

Four concrete slabs with dimensions of 600 x 500 x 200 mm were cast for this study. Two slabs were exposed to standard fire loading conditions, namely *0-8Std and 0-16Std* and two were treated as references, namely *0-8Ref and 0-16Ref*. The slabs were cured in laboratory conditions for approximately six months prior to being exposed to elevated temperature.

2.2 Fire tests

The concrete slabs were exposed to elevated temperatures using a small-scale gas-fired horizontal furnace constructed according to the test method SP Fire 119 [5]. In this

setup, a specimen is horizontally placed on top of a furnace, see Figure 1. Two edges of the specimen are supported by means of two rigid steel beams bolted together which apply a compressive load (stress of ca 2 MPa) in the longitudinal direction. At the remaining free edges of the specimen, a non-combustible insulation material fills the gap between the furnace edges and the specimen. This given setup provides the slab with a fire exposure area of 500 x 400 mm (i.e. 67 % of total area). Temperature values in the furnace and test specimen were measured using thermocouples (with a maximum temperature of less than or equal to 1100 °C). Five thermocouples were pre-installed at the center of each slab at a depth of 10, 30, 45, 80 and 120 mm. The fire load scenario studied was based on the standard temperature curve described in ISO 834-1 [3], denoted here as *Std* (Figure 2).

Figure 1: Experimental setup with specimen placed on top of the small-scale furnace [6].

At the end of the fire test, each slab was removed from the furnace and cooled down at room temperature. Eight cores with a nominal diameter of 60 mm were drilled from each slab from the fire exposed side of the test specimens, as per Figure 3. A 10 mm layer of damaged concrete was removed from the fire exposed side of the cores (underside) to negate the local effects of spalling in further testing. The specimens were sized and planned in a milling machine to a nominal length of 122.5 mm. Accordingly, the cylindrical specimens were denoted as *0-8Ref-(1-8), 0-16Ref-(1-8), 0-8Std-(1-8) and 0-16Std-(1-8)* according to the concrete mix and exposure scenario. It should be noted that only the first four specimens from each series, i.e. (1-4), were tested according to the presented measurement techniques.

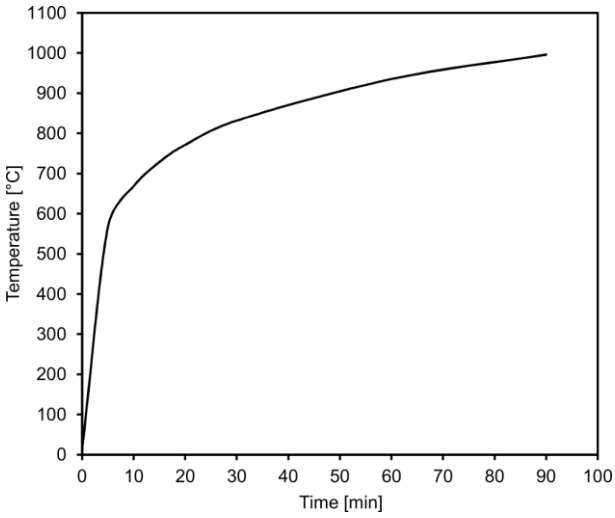

Figure 2: Standard temperature curve based on ISO 834-1 [3].

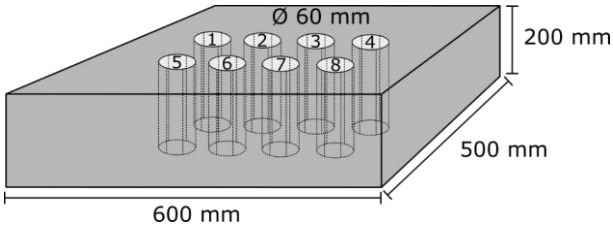

Figure 3: Geometry of slab and location of cores.

2.3 Compression tests and full-field strain determination

Uniaxial compression tests were conducted on cores drilled from the concrete slab specimens (see Figure 3). The tests were carried out in a GCTS servo-hydraulic testing machine with a stiff load frame, as shown in Figure 4. The load cell used is rated up to 1.5 MN and the accuracy of the load measurement is within 1 %. Testing was carried out under load-controlled conditions with a stress rate of 12 MPa/min. The axial

load was recorded by a load cell and the axial displacement was recorded by a linear variable differential transducer (LVDT).

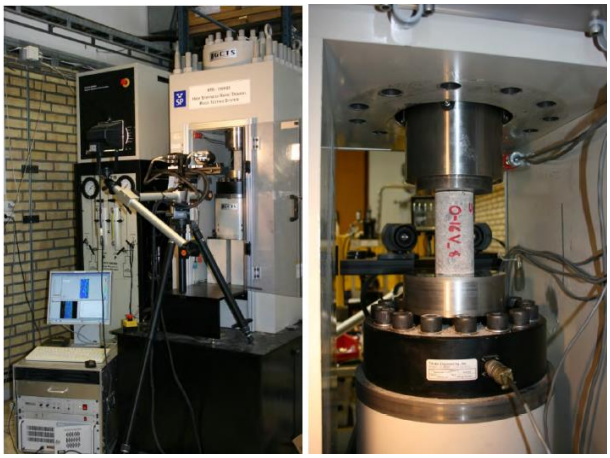

Figure 4: Experimental test setup with optical measuring system; front view (left) and back view (right) [6].

The end surface of the cores, i.e. facing the fire during testing, was placed against the lower loading plate. During loading, the strain field was monitored along one side of the core by means of full-field strain measurements using ARAMIS™ 4M (v6.2.0-6) by GOM [7]. The system applies a measurement technique based on DIC with a stereoscopic camera setup, consisting of two CCD-cameras with 4.0 Mega pixel resolutions. Essentially, DIC measures the displacement of the specimen under testing by tracking the deformation of a surface speckle pattern in a series of digital images acquired during loading. This is done by analysing the displacement of the pattern within discretized pixel subsets or facet elements of the image. By combining correlation-based stereovision techniques, the measurement of 3D shapes and displacement fields as well as of surface strain fields, is made possible.

In this study, 50 mm Schneider Macro lenses were used, and the system was calibrated for a measurement volume of 100 x 100 x 100 mm. As such, the measuring area covered a length of approximately 100 mm from the fire exposed end of the core. The natural pattern at the surface of the drilled cores was used as the speckle pattern. To obtain high contrast levels, the specimen was illuminated by a white light. An image pair captured with a frequency of 1 Hz, as well as the load and displacement from the test machine were recorded in the DIC system. A facet size of 25 x 25 px and a three-pixel overlap along the circumference of each facet were chosen, which allowed for a spatial resolution of 22 x 22 px, approximately corresponding to 0.55 x 0.55 mm. The accuracy in displacement measurements was approximately 2 μm.

3 EXPERIMENTAL RESULTS

The uniaxial compression test results of the various reference and fire exposed cores are presented to reveal the loss of compressive strength as a result of deterioration. DIC results, in the form of a strain and displacement field overlay on the tested core surface, are analyzed to ascertain the stiffness degradation of the concrete as a function of the distance from the fire exposed surface.

3.1 Compressive strength

Uniaxial compression tests were conducted on cores drilled from the concrete slab specimens (see Figure 3). Three cores from each fire exposed slab (*0-8Std* and *0-16Std*) and four cores from the unexposed slabs (*0-8Ref* and *0-16Ref*) were loaded until failure, while one core from each fire exposed slab was loaded until 20 MPa and then unloaded. The compression test results for all specimens are presented in Figure 5 as compressive stress verses axial deformation. The fire exposed specimens exhibit a lower stiffness and lower ultimate compressive strength compared to the unexposed reference specimens. More specifically, the mean compressive strength of the exposed specimens was reduced by 33 % (*0-8Std*) and 46 % (*0-16Std*).

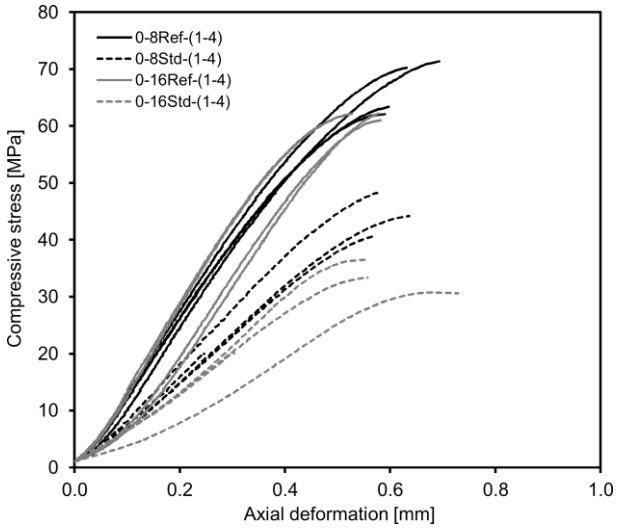

Figure 5: Comparison of compressive stress versus axial deformation for *0-8Ref*, *0-8Std*, *0-16Ref* and *0-16Std* specimens.

3.2 Stiffness degradation

In an assessment of an actual concrete structure exposed to fire, it is often more important to determine how far into the structure the concrete can be assumed to be affected than to determine actual values of the stiffness. Accordingly, the stiffness degradation along the height of a concrete core can be used to measure the level of damage caused by an elevated temperature. With DIC, it is possible to obtain a complete image of the strain field at the surface of a specimen and thus to study local effects. The optical measurements were thus analyzed in this work to determine the stiffness degradation of the concrete as a function of the distance from the fire exposed surface.

Optical measurements are exemplified in Figure 6 as an overlay of the continuous strain field at the surface of specimens *0-8Std-2* and *0-16Std-2*. The reported results are the strain in the axial direction at a compressive stress of 20 MPa. The core is orientated such that the fire exposed end is at the bottom.

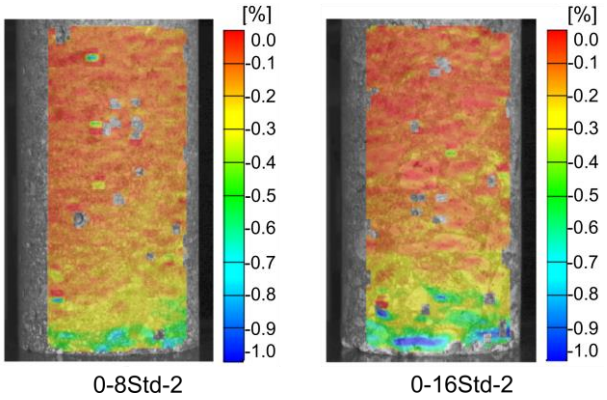

Figure 6: Overlay of axial compressive strain results at 20 MPa for *0-8Std-2* and *0-16Std-2* captured by DIC.

The strain distribution was evaluated by discretizing the core in the axial direction as illustrated in Figure 7. This method helps reduce local strain variations due to e.g. stiffness variations of the cement paste and aggregates, as well as measuring noise, see [6] for further details. The DIC measuring area was divided into nine 10 mm segments defined by ten equally spaced sections. The first section corresponds to 5 mm from the bottom surface of the core, as such the center of the first segment is comparable to 20 mm from the fire exposed surface. The axial displacement of each facet element along the sections was exported from the ARAMIS system. The strain in each segment was then calculated as the difference between the mean values of the axial displacement, $\delta_m{}^n$ and $\delta_m{}^m$, of the corresponding sections *n* and *m*, respectively, divided by the initial distance, l_0, between the sections as:

$$\varepsilon_{c,s}{}^{m\text{-}n} = (\delta_m{}^n - \delta_m{}^m)/l_0 \qquad (1)$$

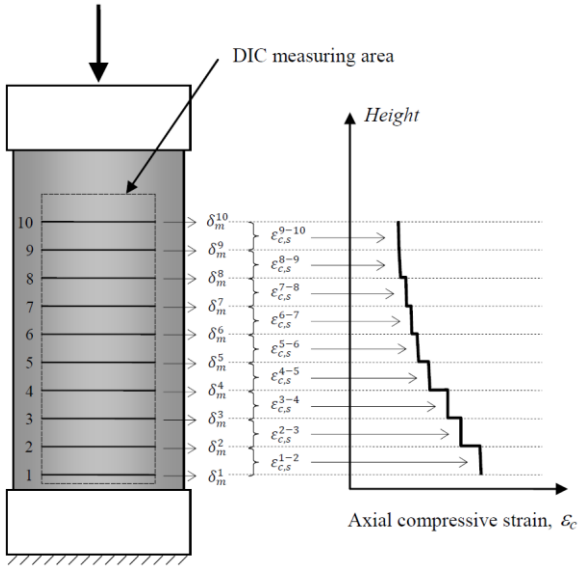

Figure 7: Schematic of evaluation of compressive strain by discretizing the DIC measuring area of the core into 10 mm segments along the height.

The distribution of the axial compressive segment strains evaluated according to the applied method is presented in Figure 8 for *0-8Ref* (mean), *0-16Ref* (mean), *0-8Std* and *0-16Std* specimens at a stress level of 20 MPa. This stress level was chosen in order to ensure comparable results within the elastic range.

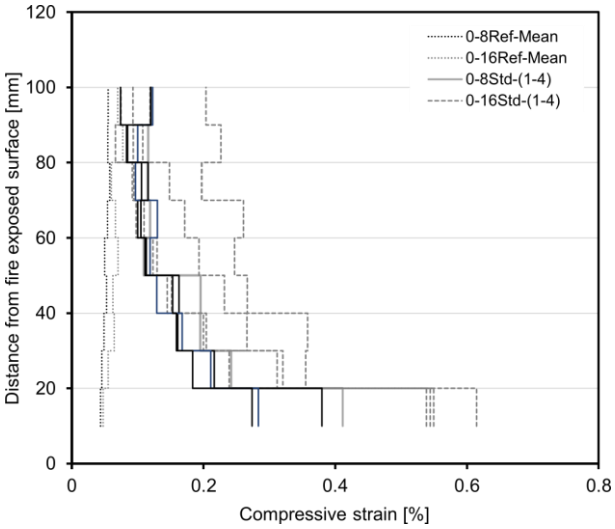

Figure 8: Axial compressive segment strains at 20 MPa for *0-8Ref (mean)*, *0-16Ref (mean)*, *0-8Std* and *0-16Std* specimens.

The mean strain distributions pertaining to the reference slabs *0-8Ref* and *0-16Ref* are relatively uniform along the height of the specimen. It can be noted that the strain values appear to be smaller closest to the bottom surface, which could be an effect of more compaction near the mould during casting.

For the fire exposed slabs, *0-8Std* and *0-16Std*, higher strain values are exhibited closest to the fire exposed surface, which is reasonable considering that these regions were exposed to the highest temperatures. With increasing distance from the fire source, the compressive strain decreases while approaching the reference strains. The highly non-uniform strain distribution for the fire exposed slabs is however observed for one *0-16Std* specimen which exhibited larger strains.

4 PREDICTIVE MODELLING

A FE model of the fire exposed concrete was developed using ABAQUS/CAE [8] to predict the change in compressive properties of the concrete due to elevated temperature. A sequentially coupled thermal stress analysis was used to solve the multiphysics problem. It is such that an uncoupled heat transfer analysis was firstly conducted followed by a stress/deformation analysis having the solved temperature field as a predefined field.

4.1 Modelling parameters

The first step of the model consisted of an uncoupled transient heat transfer analysis of a concrete section being subjected to fire loading. An axisymmetric model was defined as a 200 x 30 mm section, corresponding to the total height of the slab and nominal radius of a core sample. Diffusive heat transfer elements (4-node linear axisymmetric heat transfer quadrilateral, DCAX4) were defined on the section's surface with a mesh size of 2.5 x 2.5 mm. These elements allow for both heat storage and heat conduction.

The heat load, described by the given fire temperature curve (see Figure 2) and expected cooling curve, was applied to the bottom side of the concrete section. The heat was transferred from the combustion gas, i.e. furnace source, by means of convective and radiative heat transfer to the concrete surface. A convective heat transfer to the surrounding air was defined at the top side of the concrete section. Film

condition interactions available in ABAQUS/CAE [8] were used to describe these heat transfer mechanisms at the model surfaces, i.e. a surface film condition for convection and a surface radiation interaction for radiation.

A transient stress/deformation analysis was performed as a subsequent step in the model. The meshed section was adjusted in this step to correspond to the tested core size having a nominal height of 122.5 mm and radius of 30 mm. Axisymmetric stress elements (4-node bilinear axisymmetric quadrilateral, CAX4R) were defined for the designated section, while the mesh size, as well as the nodal and element numbering remained constant.

The maximum nodal temperatures solved via the heat transfer analysis were compiled and incorporated as a predefined temperature field for the stress analysis. A compressive pressure load was thereafter applied to the upper edge of the section to simulate the experimental compressive loading. The symmetry edge of the section was restrained against displacement along x-axis and rotations along y- and z-axes.

To accurately model the boundary conditions of the bottom nodes, the friction between the specimen and base plate would then need to be included. Alternatively, two types of boundary conditions were applied at the bottom nodes in this model: 1) restrained displacement along y-axis (BC1) and 2) restrained displacements in all directions (BC2).

4.2 Input parameters

Temperature-dependent concrete properties from EN 1992-1-2 [4] were taken as input for the predictive modelling, as these data were not experimentally quantified in the scope of this project. By doing so, a generalization of the concrete properties is included in the model, such that the 0-8 and 0-16 concrete mixes are not differentiated. Also, the influence of the PP-fibers on the properties are not incorporated.

The suitability of the available data describing the thermal properties of concrete, i.e. thermal conductivity, specific heat and density, was initially verified using the transient thermal analysis part of the model. The thermal conductivity decreases with increasing temperature as the porosity and the occurrence of micro-cracks concurrently increase. The upper limit curve for normal concrete was applied as input since it was found to yield more similar results to that of the experimentally measured thermal distribution pertaining to the applied concrete. Concerning the temperature dependent specific heat, it was observed to be most suitable to incorporate a curve corresponding to a normal concrete with 3 % moisture content. This given moisture content influences the extent of the specific heat peak between 115 and 200 °C which is related to the effect of free moisture contained in the porous system. It is also important to take into consideration the temperature dependent density which decreases with an increase in temperature due to associated moisture loss. The initial density at 20 °C was assumed to be 2400 kg/m^3 for this analysis.

At the fire exposed surface, the emissivity of concrete was taken as 0.7 in the model, which is slightly lower than the recommended 0.8 for a member in [4]. The convective heat transfer coefficient was taken as 10 W/m^{2}K at the fire exposed surface and 5 W/m^{2}K at the unexposed side facing the laboratory environment.

The temperature-dependent stress-strain curves for the concrete was calculated using mathematical models provided in [4]. The mean compressive strength of 67 MPa (ambient temperature) pertaining to *0-8Ref* concrete was applied in the calculations. Coefficients for quartz-based ballast were assumed in this case. From the calculated stress-strain curves, Young's modulus could be estimated as the slope between 20 % and 50 % of the linear stress region for temperatures between 20-1000 °C.

5 NUMERICAL RESULTS

The numerical results pertaining to the sequentially coupled thermal stress analysis of the fire exposed concrete section are presented herein. The temperature distribution captured

by the model is compared to the temperature values measured during testing. Also, compressive strains calculated from the DIC results (Section 3.2) are compared to numerical results in relation to the distance from the fire exposed surface.

A linear-elastic stress analysis was found to be suitable in this case to evaluate the adequacy of the developed model and choice of input parameters.

5.1 Thermal analysis results

To verify the outcome of the first analysis step, the temperature distribution along the height of the concrete section was compared to that measured by the thermocouples (located at 10, 30, 45, 80 and 120 mm), see Figure 9. The FEA temperature distribution presented corresponds to the nodal values at the center of the modelled section. From the figure, it can firstly be noted that the initial heating stage up to circa 600 °C differs between the applied fire load (ISO 834-1) and measured temperature in the fire. Higher measured temperatures could be related to e.g. placement of thermocouple and/or convection and radiation effects within the space between the furnace and concrete surface. Moreover, the temperature distribution becomes slightly higher than the measured values after this so-called initial heating stage (i.e. circa 10 min for 10 mm FEA, 20 min for 30 mm FEA, and 30 min for 45 mm FEA). Generally, differences between the temperature distributions are observed to diminish as the distance from the fire source increases.

In this case, the yielded numerical temperature distribution was regarded as suitable for the subsequent stress/deformation analysis, given the assumption of thermal coefficients and properties. The calculated damage of the fire exposed specimens is however expected to be marginally higher than the experimental values due to the slightly higher calculated temperature values used as input for the stress analysis.

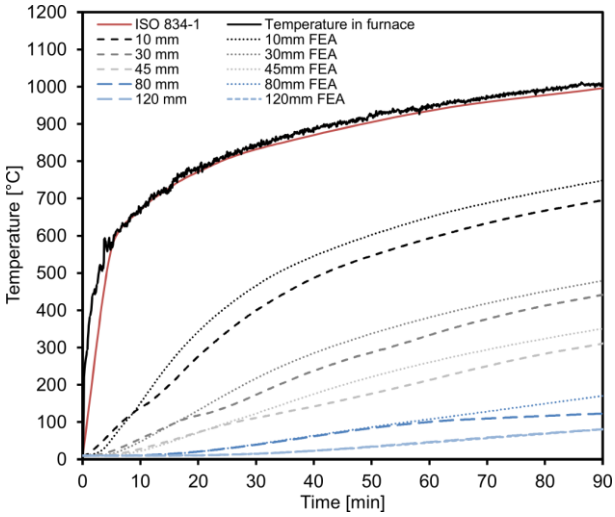

Figure 9: Temperature distribution in section with respect to time - comparison between experimental (*0-8Std*) and numerical results

A cooling curve calculated according to ISO 834-1 [3] was applied to the bottom surface of the section after 90 min of heating. Since the cooling phase was not measured during the experiment, it was of importance to incorporate the effect of heat dissipation to yield representative maximum temperatures faced by the entire concrete section. Maximum nodal temperatures, exemplified for selected heights in Figure 10, were compiled and applied as a temperature field in the stress/deformation analysis.

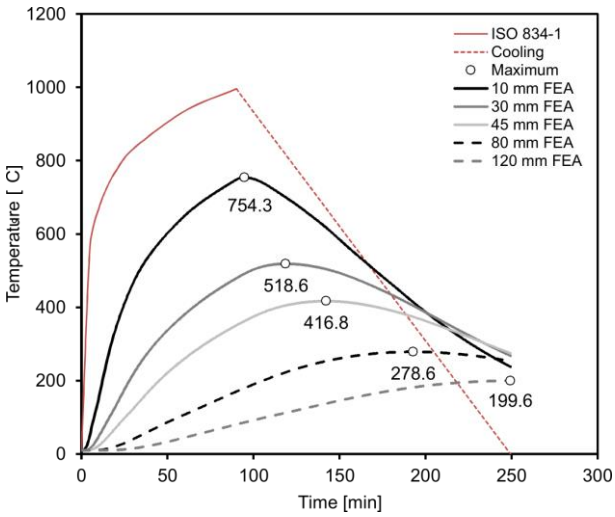

Figure 10: Maximum temperatures at selected heights in section after cooling from FEA.

5.3 Stress analysis results

The validation of the stress analysis was established by comparing the yielded compressive strain results with the segment strain distribution determined from the DIC measurements (Section 3.2). From Figure 11, it can be noted that there is a higher deviation between the FEA and experimental results at a minimal distance from the fire exposed surface, which was equally noted in the temperature analysis. However, the numerical results nevertheless have a good correlation with the *0-16Std* results particularly starting after 20 mm from the exposed surface. Moreover, differences between the assigned boundary conditions (*FEA-Std-BC1* and *FEA-Std-BC2*) are observed to be negligible.

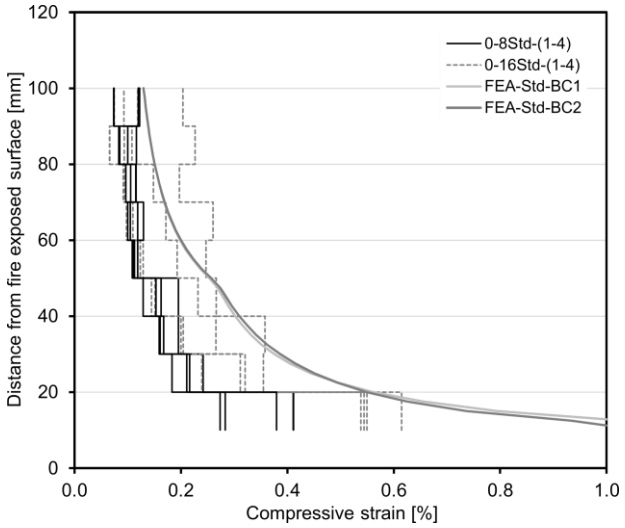

Figure 11: Change in compressive strain as a function of the distance from the fire exposed surface – comparison between experimental (*0-8Std* and *0-16Std*) and numerical results (*FEA-Std-BC1* and *FEA-Std-BC2*).

It can be concluded that the theoretical damage development based on assumed standard values for material properties correlates reasonably well with the measured damage development. With knowledge of the fire load (fire process), it could be possible to compute a theoretical assessment of the concrete's degradation from the fire exposed surface. Alternatively, if information regarding the degradation is known via drilled cores, it could be possible to predict the fire load.

6 CONCLUSIONS

A combination of optical full-field strain measurements and FEA provide a sufficiently accurate image of the fire damage development within a concrete structure along with the ability to predict the compressive properties at elevated temperatures. The theoretical results generated by this model can for instance be practical when assessing the required strengthening actions to restore the load carrying capacity and durability of the concrete structure, as well as to determine the original fire load (given input data of degradation).

However, to further improve the prediction of strength degradation, it could be worth incorporating temperature-dependent material properties obtained by means of experiments. In a realistic scenario, e.g. damage assessment of a fire exposed slab, the characterization of certain properties could be effectuated on drilled cores. By including additional measurement devices during compressive testing, i.e. strain gauges or LVDTs, the stress-strain/displacement relationship of the concrete could be further characterized. This generated data could, in turn, be applied as input for non-linear analysis and additional model validation. Furthermore, it could also be pertinent to quantify the convection and radiation coefficients related to heat transfer from the furnace to the given specimen surface.

REFERENCES

[1] Srikar, G., G. Anand, and S. Suriya Prakash, *A Study on Residual Compression Behavior of Structural Fiber Reinforced Concrete Exposed to Moderate Temperature Using Digital Image Correlation.* International Journal of Concrete Structures and Materials, 2016. **10**(1): p. 75-85.

[2] Gales, J., et al., *Fire performance of sustainable recycled concrete aggregates: mechanical properties at elevated temperatures and current research needs.* Fire Technology, 2016. **52**(3): p. 817-845.

[3] ISO 834-1, *Fire resistance tests - Elements of building constructions* 1977.
[4] EN 1992-1-2, *Eurocode 2: Design of concrete structures - Part 1-2: General rules - Structural fire design*. 2004.
[5] SP Fire 119, *Fire test of structural works in small scale (in Swedish)*. 2011, SP Technical Research Institute of Sweden SP Report 2011:19.
[6] Albrektsson, J., et al. *Assessment of fire exposed concrete with full-field strain determination*. in *2nd International RILEM Workshop on Concrete Spalling due to Fire Exposure, 2011, Delft, the Netherlands*. 2011.
[7] GOM, *GOM Correlate Manual Basic, GOM optical measuring techniques*. 2015: Braunschweig, Germany.
[8] Dassault Systèmes Abaqus/CAE User's Guide, *ABAQUS Version 6.14*. 2014.